PHILOSOPHICAL TRANSACTIONS OF THE ROYAL SOCIETY A MATHEMATICAL, PHYSICAL & ENGINEERING SCIENCES

Quantum Mechanical Predictions in Intermetallics Modelling [and Discussion]

D. Nguyen Manh, A. M. Bratkovsky, D. G. Pettifor, A. R. C. Westwood, K. S. Kumar and R. W. Cahn

Phil. Trans. R. Soc. Lond. A 1995 **351**, 529-542
doi: 10.1098/rsta.1995.0051

Quantum mechanical predictions in intermetallics modelling

By D. Nguyen Manh, A. M. Bratkovsky and D. G. Pettifor
Department of Materials, University of Oxford, Parks Road, Oxford OX1 3PH, UK

Materials modelling involves research that spans the very broad spectrum of length scales from quantum mechanical calculations at the Å level all the way through to finite-element or finite-difference modelling at the continuum level. This paper reviews the role that quantum mechanics plays in the modelling hierarchy with particular reference to the titanium and nickel aluminides.

1. Introduction

The prediction of the properties of high-temperature intermetallics involves research that spans the very broad spectrum of length scales from quantum mechanical calculations at the Å level all the way through to finite-element or finite-difference modelling at the continuum level. The spectrum divides naturally into four different hierarchies or levels, namely the electronic, atomistic, microstructural, and continuum as shown in figure 1. We can loosely think of these as embracing the domains of the physicist and chemist (the solution of the Schrödinger equation and the nature of the chemical bond describing the interaction between the atoms respectively), the materials scientist (the evolution of microstructure), and the engineer (the modelling of processing). In this paper we are interested in bridging the gap between the electronic and atomistic hierarchies. In a following paper Rappaz (this volume) will address the question of how the gap is bridged between the microstructural and continuum hierarchies.

In intermetallics the unsaturated covalent bonds between different atomic species result in several important properties. First, perhaps the most important, they tend to be very strong and stiff, their strength and stiffness being maintained up to high temperature. Morever, some intermetallics such as Ni_3Al show an anomalous sharp rise in strengh with increasing temperature. Such a unique property makes intermetallics even more attractive as high-temperature materials. Second, they often show good oxidation resistance. For example, in the case of NiAl which has a higher melting point than those of the constituent elements, strong bonds between aluminium and nickel make their aluminium reservoir stable up to a high temperature and result in a remarkable high-temperature oxidation resistance. Third, those compounds based on light elements, such as TiAl and Ti_3Al, can have very low densities. The low density combined with the high strength and stiffness give rise to very attractive specific properties, which are especially important for rotating machinery and aerospace applications (Yamaguchi & Inui 1993). Unfortunately, at the same time, the directional nature of

Phil. Trans. R. Soc. Lond. A (1995) **351**, 529–542
Printed in Great Britain

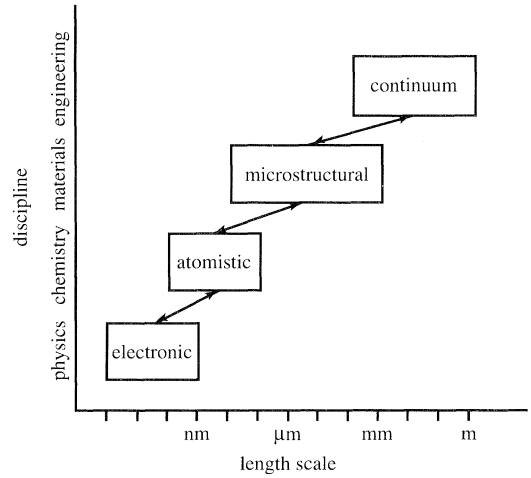

Figure 1. Hierarchy of models in materials research.

the covalent bond between different atomic species tends to cause intermetallics to be brittle at low temperatures. Therefore they are unlikely to find extensive engineering application, unless ways can be found to overcome this brittleness. Because of their great promise, there is a lot of effort to understand the origin of their brittleness.

A fundamental study of the deformation behaviour of intermetallics requires a realistic description of the bonding between the different constituent atoms. Simple pair potentials or the more recently developed embedded atom or Finnis–Sinclair potentials cannot explain the origin of the brittleness since the explicit *directional* character of the bonding is neglected. To solve this problem we are required to bridge the gap between the electronic and atomistic levels in the modelling hierarchies and to derive interatomic potentials that are firmly based on the quantum mechanical predictions of the Schrödinger equation. Recently, a novel angular-dependent interatomic potential has been obtained within the two-centre tight-binding approximation in which the directional character of the bonding is included explicitly from the outset (Pettifor 1989). Moreover, the many-atom expansion for this so-called bond order potential (BOP) has been shown to be not only exact but also rapidly convergent (Aoki 1993). The BOP scheme is an $O(N)$ method, in which the number of arithmetic operations grows *linearly* with the system size N. The BOPs may be used therefore for the atomistic modelling of very large systems in the studies of defects such as dislocation cores and interfaces.

The development of the BOP for a given system requires the appropriate tight-binding parameters as input. Since the two-centre, orthogonal tight-binding approach is semi-empirical the tight-binding parameters and their distance dependence must be *fitted* to theoretically predicted local density functional band structure and binding energy curves of both the ground state and metastable phases, as has been done with great success for silicon (Goodwin *et al.* 1989).

The purpose of this paper is to make a systematic first-principles study of the bonding of the 3d and 4d transition metal aluminides and to generate an *ab initio* database by solving the Schrödinger equation at the electronic level. Particular attention will be paid to possible competing phases with respect to the

ground state structures $L1_0$ for TiAl and B2 for NiAl which are the promising candidates for new high-temperature structural materials (Darolia 1991; Dimiduk 1992). This database will then be used to fit reliable transferable tight-binding parameters for TiAl and NiAl to perform defect simulations at the atomistic level using the novel angularly dependent BOPs (Pettifor *et al.* 1995).

2. Ab initio binding energy database

(*a*) *Local density functional theory*

Application of electron theory to understanding and predicting the properties of metals and alloys needs a reliable method for computing the stability of an arbitrary collection of atomic nuclei and electrons from first principles, that is, without resorting to experimental input other than universal constants. As one of the first-principles approaches, density functional theory is an exact theory for the total ground state energy of a system of electrons and fixed nuclei (Hohenberg & Kohn 1964; Kohn & Sham 1965). Within the so-called local density approximation (LDA), the exchange-correlation energy density is assumed to be that of a homogeneous electron gas with the same density as that seen locally by the electron. The total LDA energy is then a unique functional of the electron density $n(\boldsymbol{r})$, namely

$$U_{\mathrm{T}}[n] = \sum_{i,\mathrm{occ}} E_i - \frac{1}{2}\iint \mathrm{d}\boldsymbol{r}\mathrm{d}\boldsymbol{r}' \frac{n(\boldsymbol{r})n(\boldsymbol{r}')}{|\boldsymbol{r}-\boldsymbol{r}'|} - \int \mathrm{d}^3r\, n(\boldsymbol{r})\mu_{xc}(\boldsymbol{r}) + U_{xc}[n] + U_{\mathrm{ion-ion}}. \tag{2.1}$$

The first contribution, the band energy, is the sum of occupied eigenvalues E_i obtained by solving the one-electron Schrödinger equation with an effective potential V_{eff} given by

$$V_{\mathrm{eff}}(\boldsymbol{r}) = V_{\mathrm{ext}}(\boldsymbol{r}) + \int \mathrm{d}\boldsymbol{r}' \frac{n(\boldsymbol{r}')}{|\boldsymbol{r}-\boldsymbol{r}'|} + \mu_{xc}(\boldsymbol{r}). \tag{2.2}$$

V_{eff} comprises three terms: the external potential due to the positive nuclei, the averaged electrostatic potential of the electron gas or Hartree potential, and the exchange-correlation potential (which is the functional derivative of U_{xc} with respect to n). The electronic density can be constructed from the eigenfunctions $\psi_i(\boldsymbol{r})$ of the Schrödinger equation by using

$$n(\boldsymbol{r}) = \sum_{i,\mathrm{occ}} |\psi_i(\boldsymbol{r})|^2. \tag{2.3}$$

The second, third and fourth contributions to (2.1) correct for the double-counting of the electrostatic and exchange-correlation energies, respectively, because the eigenvalue E_i contains the potential energy of interaction with the jth electron and vice versa. The last contribution represents the ion–ion Coulomb interaction.

All the calculated results using self consistent LDF theory must be regarded as essentially the solution to the many-body quantum mechanical problem of a system of electrons and nuclei in a solid. The solution of the one-electron Schrödinger equation can be obtained numerically through one or other of the many, well developed band structure methods. They involve expanding the eigenfunctions $\psi_i(\boldsymbol{r})$ in basis set functions (e.g. plane-waves, muffin-tin orbitals, etc.). The cal-

PHILOSOPHICAL TRANSACTIONS OF THE ROYAL SOCIETY A MATHEMATICAL, PHYSICAL & ENGINEERING SCIENCES

Table 1. *Characterization of twelve different structure types*

structure		spacegroup		local coordination
$L1_0$	CuAu	P4/mmm	123	(8Al+4TM) + 6TM
40	Kanamori	$I4_1/amd$	141	(8Al+4TM) + (2Al+4TM)
$L1_1$	CuPt	$R\bar{3}m$	166	(6Al+6TM) + 6Al
B19	AuCd	Pmma	51	(8Al+4TM) + 6TM
B2	CsCl	$Pm\bar{3}m$	221	8Al + 6TM
B32	NaTl	Fd3m	227	(4Al+4TM) + 6Al
B11	CuTi	P4/nmm	129	(4Al+4TM) + (2Al+4TM)
B33	CrB	Cmcm	63	7Al + 10TM
B20	FeSi	$P2_13$	198	7Al + 6TM
B27	FeB	Pmna	62	7Al + 10TM
$B8_1$	NiAs	$P6_3/mmc$	194	(6Al+2TM) +6TM
B1	NaCl	Fm3m	225	6Al + 12TM

culations in this section are made by using the full-potential linear muffin-tin orbitals (FP-LMTO) method (Methfessel 1988) which provides the smallest basis set with a precision of about 10^{-4} Ry for the total energy U_T. This accuracy is needed for determining structural energy differences which are often of the order of mRy per atom. Since the total energy U_T is of the order of 10^4 Ry per atom this requires a convergence of 1 part in 10^7.

(*b*) *Binding energy curves*

In this study the choice of the competing structure-types within the transition metal aluminides is guided by the two dimensional AB structure maps where the observed ground state structures of neighbouring AB compounds to TiAl and NiAl are displayed (Pettifor 1992). We find, as expected, that TiAl takes the tetragonal $L1_0$ (CuAu) structure type which, neglecting the tetragonal distortion, results from ordering the titanium and aluminium atoms with respect to an underlying FCC lattice so that each atom is surrounded by a local coordination polyhedron of twelve atoms. On the other hand, we find that NiAl takes the cubic B2 (CsCl) structure type which results from ordering the nickel and aluminium atoms with respect to an underlying BCC lattice so that each atom is surrounded by a local coordination polyhedron of fourteen atoms comprising eight first and six second nearest neighbours. Importantly we find that if the 3d element Ti is replaced by isovalent 4d-Zr or 5d-Hf then the most stable structure is not tetragonal CuAu but orthorhombic CrB. Similarly, we find if the 3d element Ni is replaced by isovalent 4d-Pd or 5d-Pt then the most stable structure is not cubic CsCl but cubic FeSi with only seven unlike nearest neighbours in a distorted first neighbour shell rather than the eight of CsCl.

In our investigations, we have included the twelve different structure types listed in table 1. We have grouped these structure according to whether they are close packed FCC-like, HCP-like, BCC-like or some other more open structure type, respectively. For FCC-like structures, the following structures were included: $L1_0$ (CuAu), $L1_1$ (CuPt) and 40 (Kanamori phase) which correspond to stars

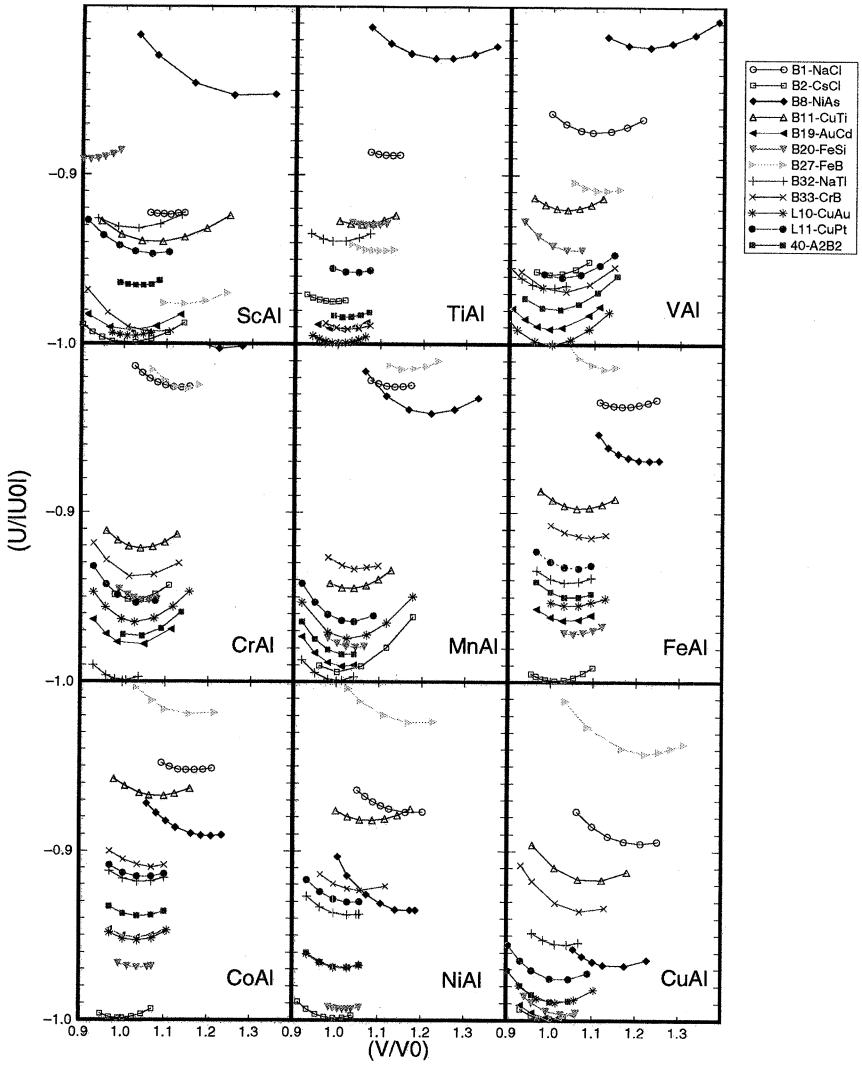

Figure 2. Self-consistent FP-LMTO binding energy-volume curves amongst the 3d transition metal aluminides with respect to twelve different structure types.

$\langle 100\rangle$, $\langle \frac{1}{2}, \frac{1}{2}, \frac{1}{2}\rangle$ and $\langle 1, \frac{1}{2}, 0\rangle$ respectively within the FCC Brillouin zone. For HCP-like structures, we included the only one that is observed for AB compound structures, namely B19 (AuCd). For the BCC-like structures, we include the B2 (CsCl), B32 (NaTl) and B11 (γ-CuTi) structures which correspond to the stars $\langle 100\rangle$, $\langle \frac{1}{2}, \frac{1}{2}, \frac{1}{2}\rangle$ and $\langle \frac{1}{2}, \frac{1}{2}, 0\rangle$, respectively, within the BCC Brillouin zone. The other structures we included are: B1 (NaCl), $B8_1$ (NiAs), B20 (FeSi), B27 (FeB) and B33 (CrB) which are commonly occuring structure types for the pd-bonded AB compounds (Pettifor & Podloucky 1986). The local coordination polyhedron that surrounds each transition metal atom is given in the last column of table 1 for each structure-type. The details of the FP-LMTO calculations for all the 3d and 4d transition metal aluminides will be analysed elsewhere. Here we give only some results concerning the prediction of structural trends within the transition metal aluminide compounds.

Table 2. *Equilibrium volume per unit formula and bulk modulus of ground state for 3d and 4d transition metal aluminides*

(B_{theor} is the result from other first-principle calculation.)

material (structure)	volume/Å^3		bulk modulus/Mbar	
	V_{cal}	$V_{\mathrm{cal}}/V_{\mathrm{exp}}$	B_{cal}	(B_{exp} or B_{theor})
ScAl-(B2)	38.96	0.95	0.62	—
TiAl-($L1_0$)	30.96	0.95	1.29	1.26
VAl-($L1_0$)	27.20	—	1.59	—
CrAl-(B32)	24.56	—	1.89	—
MnAl-(B32)	23.39	—	1.91	—
FeAl-(B2)	22.99	0.94	1.88	1.52,1.83
CoAl-(B2)	22.19	0.95	1.92	1.62
NiAl-(B2)	22.90	0.96	1.84	1.57,1.87,1.93
CuAl-(C2/m)	26.98	0.96	1.65	—
YAl-(B33)	47.41	0.97	0.66	—
ZrAl-(B33)	37.93	0.98	1.08	—
RuAl-(B2)	26.19	0.94	2.23	2.20
RhAl-(B2)	25.93	0.97	2.16	—
PdAl-(B20)	28.11	0.98	2.07	—

The complete set of binding energy curves for the 3d transition metal aluminides is given in figure 2 where the curves plotted have been scaled with respect to the calculated energy and volume of the most stable structure. We see that the ground states of the observed transition metal aluminides are predicted correctly: ScAl in the B2 structure, TiAl in the $L1_0$ structure, FeAl, CoAl and NiAl in the B2 structure. The B2 structure is shown in this figure to be most stable for CuAl as well, but this phase in fact is predicted to become unstable with respect to the monoclinic phase C2/m, which has a binding energy of about 4 mRy per atom lower than the B2 phase. If vanadium and chromium aluminides were to exist in the 50–50 stoichiometry then we would predict VAl to be $L1_0$ whereas CrAl would be B32. We predict that ferromagnetic state of $L1_0$–MnAl is more stable than nonmagnetic B32 which is also consistent with experimental observation (see, for example, Zhang & Soffa 1994).

In table 2 we give the calculated equilibrium volume and bulk modulus of the ground state for 3d and 4d transition metal aluminides. We see that the theoretial predictions compare very well with the experimental data where available. As expected, the lattice expands when going from 3d to 4d transition metal aluminides. The structural stability of the transition metal aluminides is presented in figure 3 where the structural energy difference relative to B2 is plotted as a function of the average number of valence electron per atom. We note that the changes in energy ΔU between competing structure-types are indeed varying from 10^{-3} to 10^{-2} Ry per atom as mentioned in the previous section. We find the structural trend from B2 (BCC-like) to $L1_0$ (FCC-like) to B19 (HCP-like) to B2 (BCC-like) as function of the average number of electrons per atom. This trend is different

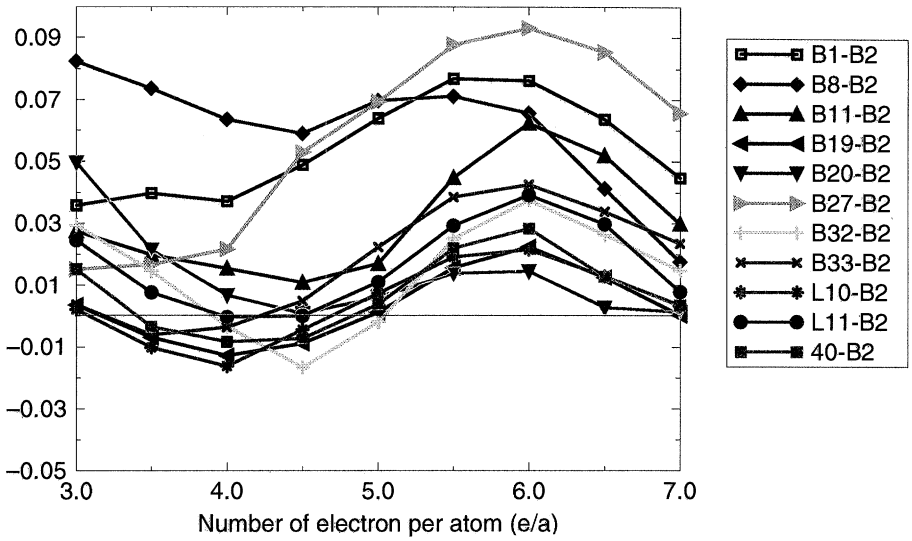

Figure 3. Structural energy differences relative to the B2 structure for the 3d-transition metal aluminides.

from that for the pure nonmagnetic transition metals where we go from HCP to BCC to HCP to FCC across the series. Thus, the structural stability depends on the angular character of the valence orbitals taking part in the bonding. We will explain the origin of the structural trend across the transition metal aluminides in the next subsection.

(*c*) *Focus on* TiAl *and* NiAl

Titanium aluminide and nickel aluminide are the two representative compounds at the beginning and end of the transition metal aluminides. The binding energy curves of these two compounds and also those of corresponding 4d compounds ZrAl and PdAl are shown in figure 4. We see that B33 (CrB) is predicted to be the closest metastable phase to the $L1_0$ ground state of TiAl, being about 3 mRy per atom higher in energy. Other nearby competing phases are B19 (AuCd), an ordered structure type with respect to the HCP lattice, being 3.4 mRy per atom higher in energy and the Kanamori phase labelled 40 which is an ordered structure type with respect to the FCC lattice. We observe that the LDA calculations predict correctly that ZrAl take the B33 (CrB) structure with $L1_0$ as the closest metastable phase. On the other hand, at the end of a series we see that B20 (FeSi) is the closest metastable phase to the B2 ground state of NiAl, being only about 3 mRy per atom higher in energy. Again when the 3d-Ni is replaced by isovalent 4d-Pd, our LDA calculations predict correctly that PdAl takes the B20 (FeSi) structure type with B2 as the closest metastable phase.

The prediction that the B33 and B20 structure-types are the nearest competing phases to the $L1_0$ of TiAl and the B2 of NiAl, respectively, is interesting because the structural stability of these phases is determined explicitly by the directional d(TM)-p(Al) bonding which is well described by the tight-binding model (Pettifor & Podloucky 1986). A dramatic example of the importance of directional bonding in determining intermetallic structure and properties is provided by $RuAl_2$ which takes the $TiSi_2$ structure type. This intermetallic was predicted to be a semicon-

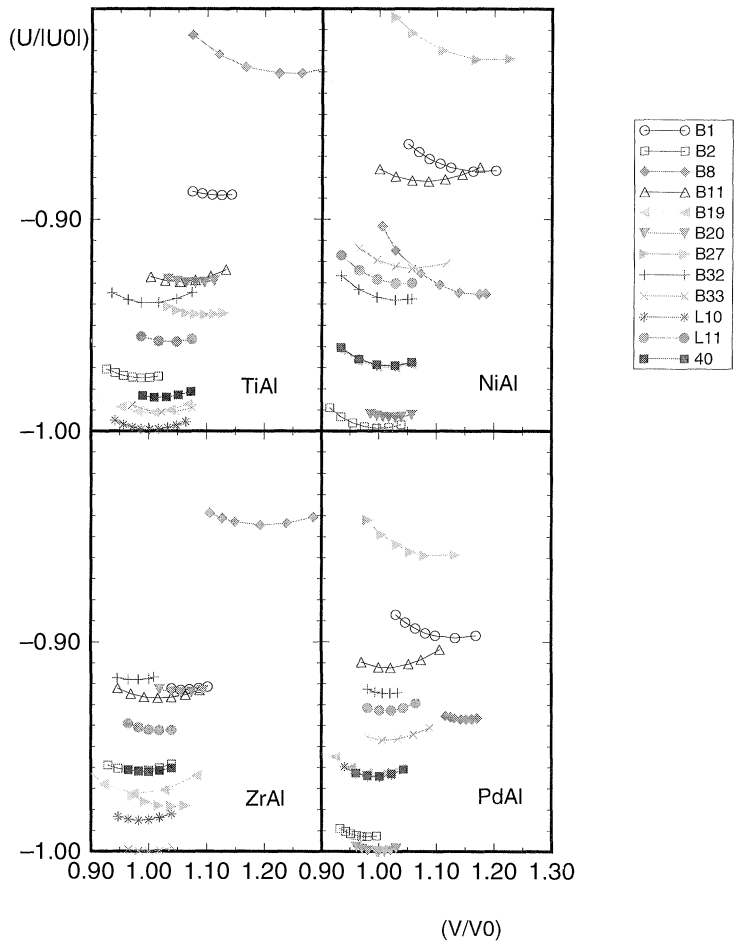

Figure 4. Binding energy curves for TiAl, NiAl, ZrAl and PdAl with respect to twelve different structure types.

ductor with the hybridization gap resulting directly from the angular character of pd bonding orbitals which separates the pd bonding from pd antibonding states, a theoretical result (Nguyen Manh *et al.* 1992) later confirmed by experiment (Pierce *et al.* 1993).

The structural stability in these phases is controlled mainly by the band structure energy contribution in (2.1) whose magnitude depends on the shape of the density of states. Figures 5*a*–*c* show the densities of states of the three competing phases $L1_0$, B33 and B19, respectively, at the fixed equilibrium volume for titanium aluminide from which we can deduce the relative stability within a non-self-consistent 'frozen-potential' approach (Nguyen Manh *et al.* 1995). It is clear that the hybridization between Ti and Al states has a very *similar* character for the three competing structures. The same conclusion can be made from figures 5*d*, *e* where the calculated density of states for the ground state B2 and its competing metastable phase B20 are shown.

An estimate of the energy difference between two structures can be obtained

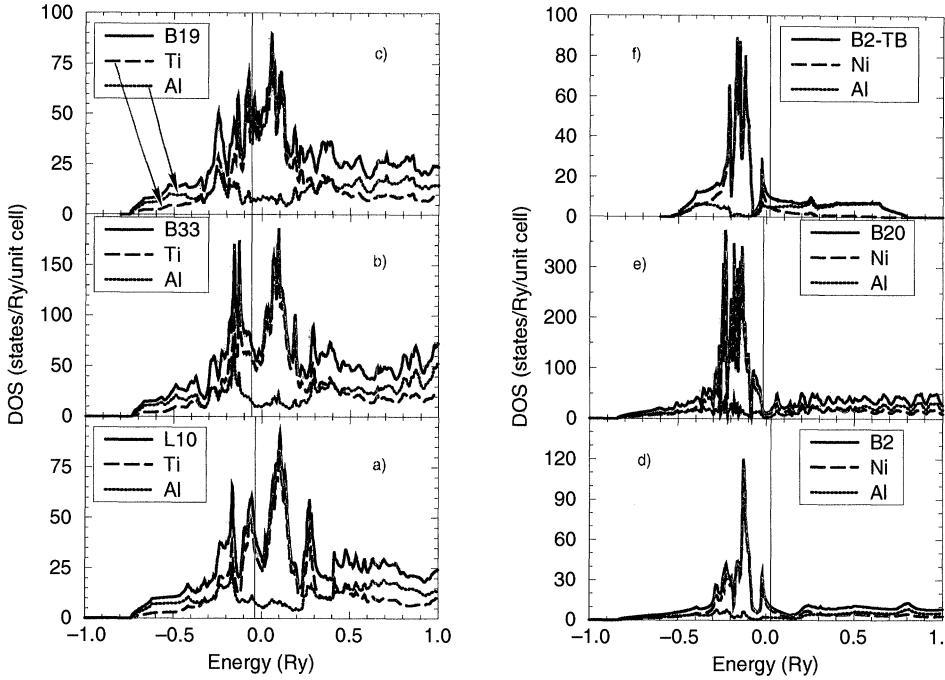

Figure 5. The calculated density of states for TiAl in the three competing phases: (*a*) $L1_0$, (*b*) B33 and (*c*) B19. The calculated density of states for NiAl in the two competing phases: (*d*) B2 and (*e*) B20. (*f*) Tight-binding density of states for NiAl in the p(Al)-d(Ni) model.

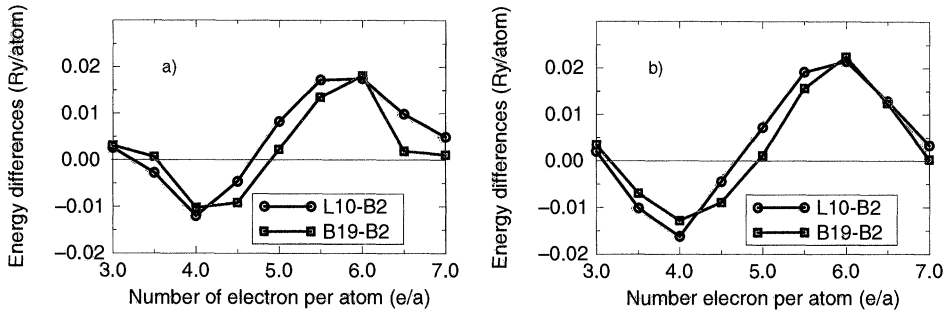

Figure 6. Structural energy differences between B19 and $L1_0$ relative to B2 calculated from (*a*) the B2-NiAl 'frozen-potentials' and (*b*) FP-LMTO method.

by comparing their band structure energies at the same atomic volume, namely

$$\Delta U_{\mathrm{T}} \approx \Delta U_{\mathrm{b}} = \Delta \left[\int^{E_{\mathrm{F}}} En(E)\,\mathrm{d}E \right], \tag{2.4}$$

where E_{F} is the Fermi energy and $n(E)$ is the total electronic density of states.

Figure 6*a* shows the band energy differences between the HCP-like B19 and the FCC-like $L1_0$ structures compared to BCC-like B2 for the NiAl densities of states. We see that the structural energy differences are very similar to those obtained from the self-consistent FP-LMTO calculation in figure 6*b*. Very importantly, these calculations show that the band structure energy is a dominant factor in deter-

mining the structural stability of the transition metal aluminides. This factor is entirely quantum mechanical in origin.

3. Bond order potentials

(a) *Many-atom expansion for the bond order*

Within the two-centre orthogonal tight-binding approximation the covalent bond energy $U^{ij}_{\rm bond}$ between sites i and j may be written explicitly as (Pettifor 1989)

$$U^{ij}_{\rm bond} = H_{ij}\Theta_{ji}(E_{\rm F}), \tag{3.1}$$

where H_{ij} is the tight-binding Hamiltonian matrix linking sites i and j and $\Theta_{ji}(E_{\rm F})$ is the *bond order* (Coulson 1939). The bond order is the difference between the number of electrons in the bonding and antibonding states, respectively. It is a *non-pairwise* quantity since it depends on the local atomic environment about the bond and can be expressed *exactly* via the *moments of tight-binding Hamiltonian* as a many-atom expansion (Pettifor 1989; Aoki 1993).

The simplest approximation to the bond order retains only the first term in the many-atom expansion. This contribution takes into account the *second moment* only and gives immediately the embedding function introduced by Finnis & Sinclair (1984) in their embedded-atom potentials. The second moment about atom i can be written

$$\mu_2 = \sum_{j\neq i} H_{ij}H_{ji} = \sum_{j\neq i} H^2(R_{ij}). \tag{3.2}$$

The square root of the second moment is a measure of root mean square band width of the local density of states on atom i. The second term in the many-atom expansion for the bond order is dependent on the third moment μ_3 which sums over all the three-member ring contribution of type $i \longrightarrow j \longrightarrow k \longrightarrow i$. This accounts for the asymmetric behaviour or skewing of the local density of states. The third term in the expansion is dependent on the fouth moment μ_4 which sums over paths sush as the four member ring contribution $i \longrightarrow j \longrightarrow k \longrightarrow l \longrightarrow i$. The fourth moment defines the unimodal or bimodal shape of the density of states (see, for example, Bratkovsky *et al.* 1994).

The BOP formalism is an order N method, the computational time varying linearly with the number of atom N simulated. It is, therefore, significantly faster when applied to large systems than the methods using direct diagonalization of the Hamiltonian matrix where the time scales as the third power of the number of atoms N in the cell.

(b) *Application for* TiAl *and* NiAl

To develop the angularly dependent BOPs for transition metal aluminides, the *ab initio* binding energy curves are used to fit reliable transferable TB parameters.

(i) *Titanium aluminide*

Titanium has partially filled d-bands so that the atoms are non-spherical and the bonding is expected to display angular character. We first develop the BOP for elemental HCP-titanium using canonical tight-binding hopping intergrals

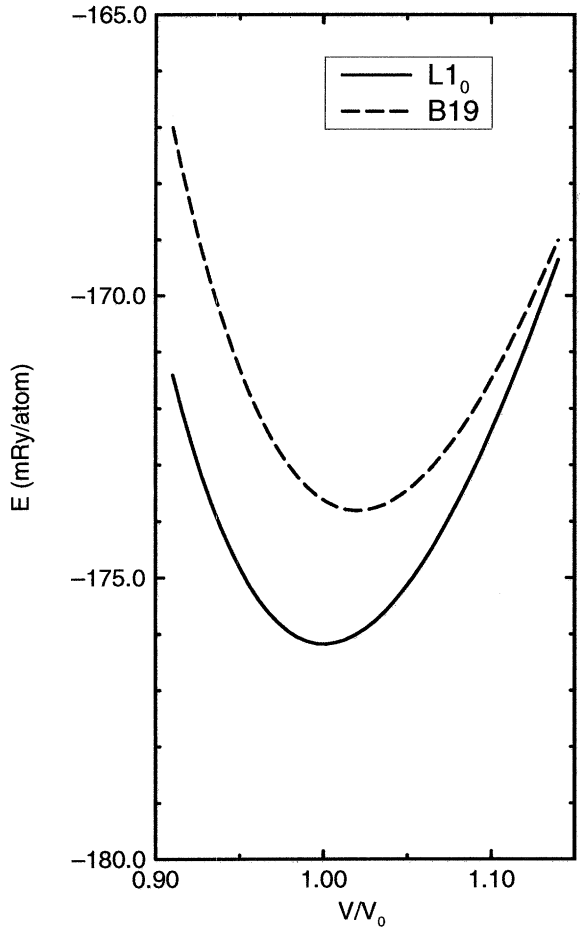

Figure 7. The binding energy curves from tight-binding model for TiAl for $L1_0$ and B19 structures.

ddσ:ddπ:ddδ $= -6 : 4 : -1$. This potential correctly reproduces the *ab initio* structural energy-volume curves for HCP, FCC and BCC Ti within the sixth-moment approximation to the density of states. We then developed the BOP for *compound* TiAl. As stressed above directional bonding plays an important role in the structural stability of the group IV transition metal aluminides: whereas TiAl takes the $L1_0$ structure, ZrAl and HfAl take the complicated phase B33 structure (CrB type). This structure and the HCP-like B19 are the closest metastable phases to the $L1_0$ ground state of TiAl. Figure 5*a* shows that the Fermi level of TiAl is positioned in the middle of the d-band of Ti where the hybridization between the d(Ti) and the p(Al) states is strong. This situation is not captured by Embedded Atom type potentials. Figure 7 shows the tight-binding binding energy curves of TiAl with respect to the $L1_0$ and B19 using canonical parameters ppσ:ppπ $= 2 : -1$ and pdσ:pdπ $= -3 : 3^{1/2}$. The transferrable tight-binding BOP gives the energy difference between $L1_0$ and B19 as 3.5 mRy per atom in good agreement with the *ab initio* calculations. We are currently predicting the binding energy curves for the other structure types of TiAl in figure 2.

(ii) *Nickel aluminide*

Unlike titanium the d-band of nickel is nearly full. The electronic density of states of nickel aluminide (figure 5*d*) shows that the Fermi level is positioned at the top of this d band, so that, the bonding is expected to have more spherical character than for the titanium aluminides. Nevertheless, there are two points which make us to believe that the angular bonding is still important in this intermetallic. Firstly, a very simple tight-binding calculation in which only the p orbitals on Al and d orbitals on Ni are retained, reproduces very well the shape of the density of states for B2-NiAl as shown in figure 5*f*. Thus, the particular shape of the density of states in NiAl can be explained by the strong covalent bonding between Ni and Al. Secondly, we note that PdAl takes the B20 structure type which is a distorted CsCl type lattice. Pd has the same number of d-electrons as Ni but PdAl takes the complex FeSi structure due to the covalent directional Al(p)-Pd(d) bonding. The directionality of the bonding is responsible for the B20 structure type being the closest metastable phase for NiAl. Preliminary results from BOPs calculations for NiAl show that these speculations are correct, as will be described elsewhere.

4. Conclusions

We have demonstrated the importance of a proper quantum mechanical description of the bonding for understanding the structural properties of the transition metal aluminides. In particular, we have shown that the closest competing structures types to the $L1_0$ ground state of TiAl and the B2 ground state of NiAl are the B33 (CrB) and B20 (FeSi) phases, respectively. The structural stability of these metastable phases is determined by the directional pd bonding between the sd-valent transition element and sp-valent aluminium.

Reliable atomistic simulation of the defect properties of the transition metal aluminides, therefore, requires the development of angularly dependent interatomic potentials. We have shown how it is possible to bridge the gap between the first principles quantum mechanical calculations at the *electronic* level and the simulations of defects at the *atomic* level by using the novel many-atom expansion for the bond order within the tight-binding description of the electronic properties. These potentials have been fitted to the band structure and binding energy curves of TiAl and NiAl and will be used in the near future for simulating defects in these intermetallics.

We are very grateful to Dr Tony Paxton for his help with the FP-LMTO calculations and many helpful discussions during this work. D.N.M. thanks the Japanese NEDO project for financial support, A.M.B. thanks the EPSRC. Computations were performed in the Materials Modelling Laboratory, Department of Materials, Oxford, which has been funded in part by the EPSRC under grant GR/H 58278-C80 and on SERC's Cray Y-MP at Rutherford Appleton Laboratory.

References

Aoki, M. 1993 Rapidly convergent bond order expansion for atomistic simulations. *Phys. Rev. Lett.* **71**, 3842–3845.

Bratkovsky, A. M., Aoki, M., Horsfield, A. & Pettifor, D. G. 1994 Tight-binding calculations in real space: towards the bond-order potentials. Workshop on Bond-Order Potentials for Atomistic Simulations, University of Oxford, Oxford, 26–27 September.

PHILOSOPHICAL TRANSACTIONS OF THE ROYAL SOCIETY A MATHEMATICAL, PHYSICAL & ENGINEERING SCIENCES

Coulson, C. A. 1939 The electronic structure of some polyelenes and aromatic molecules. VII. Bonds of fractional order by molecular orbital method. *Proc. R. Soc. Lond.* A **169**, 413–428.

Darolia, R. 1991 NiAl alloys for high-temperature structural appications. *J. Metals* **43**, 44–49.

Dimiduk, D. M., Miracle, D. B. & Ward, C. H. 1992 Development of intermetallic materials for aerospace systems. *Mater. Sci. Technol.* **8**, 367–375.

Finnis, M. W. & Sinclair, J. E. 1984 A simple empirical N-body potential for transition metals. *Phil. Mag.* A **85**, 45–55.

Goodwin, L., Skinner, A. J. & Pettifor, D. G. 1989 Generating transferable tight-binding parameters: application to silicon. *Europhys. Lett.* **9**, 701–706.

Hohenberg, P. & Kohn, W. 1964 Inhomogeneous electron gas. *Phys. Rev.* **136B**, 864–871.

Kohn, W. & Sham, L. 1965 Self-consistent equations including exchange and correlation effect. *Phys. Rev.* **140A**, 1133–1138.

Methfessel, M. 1988 Elastic constants and phonon frequencies of Si calculated by a fast full-potential linear-muffin-tin-method. *Phys. Rev.* **38B**, 1537–1540.

Nguyen Manh, D., Paxton, A. T., Pettifor, D. G. & Pasturel, A. 1995 On the phase stability of transition metal trialuminides compounds. *Intermetallics* **3**, 9–14.

Nguyen Manh, D., Trambly de Lassardiere, J. J. P., Mayou, D. & Cyrot-Lackmann, F. 1992 Electronic structure and hybridization effect in the compounds Al_2Ru and Ga_2Ru. *Solid St. Commun.* **82**, 329–334.

Pettifor, D. G. 1989 New many-body potential for the bond order. *Phys. Rev. Lett.* **63**, 2480–2843.

Pettifor, D. G. 1992 Theoretical predictions of structure and related properties of intermetallics. *Mater. Sci. Technol.* **8**, 345–349.

Pettifor, D. G., Aoki, M., Gumbsh, P., Horsfield, A., Nguyen Manh, D. & Vitek, V. 1995 Defect modelling: the need for angularly-dependent potentials. *Mater. Sci. Engng* A **192/193**, 24–30.

Pettifor, D. G. & Podloucky, R. 1986 The structure of binary compounds. II. Theory of the pd-bonded AB compounds. *J. Phys.* C **19**, 315–330.

Pierce, F. S., Poon, S. J. & Biggs, B. D. 1993 Band-structure gap and electronic transport in metallic quasicrystals and crystals. *Phys. Rev. Lett.* **70**, 3919–3922.

Yamaguchi, M. & Inui, H. 1993 TiAl compounds for structural applications. *Structural intermetallics* (ed. R. Darolia, J. J. Lewandowski, C. T. Liu, P. L. Martin, D. B. Miracle & M. V. Nathal), pp. 127–142. The Minerals, Metals and Materials Society.

Zhang, B. & Soffa, W. A. 1994 The structure and properties of $L1_0$ ordered ferromagnets: Co–Pt, Fe–Pt, Fe–Pd and Mn–Al. *Scr. metall. Mater.* **30**, 683–688.

Discussion

A. R. C. Westwood (*Sandia National Laboratories, USA*). What are the prospects for extending this approach to ternary and quaternary alloys with the ultimate objective of developing, from first principles, an intermetallic that exhibits significant ductility?

D. G. Pettifor. The approach of modelling defects using bond order potential is easily extendable to a treatment of ternary and quaternary alloys provided the appropriate tight binding parameters between the different chemical constituents are known. These calculations at the electronic and atomistic level would have to be linked to simulation of dislocation behaviour at the microstructural level before we have a truly 'first principles' modelling capability of ductile behaviour.

K. S. Kumar (*Martin Marietta Laboratories, Baltimore, USA*). Given that the mechanical properties of intermetallic compounds are particularly sensitive to minor stoichiometric deviations as well as minor alloying additions, how realistically

PHILOSOPHICAL TRANSACTIONS OF THE ROYAL SOCIETY A MATHEMATICAL, PHYSICAL & ENGINEERING SCIENCES

can we expect atomistic modelling to serve as a predictive tool, since the number of atoms/cells that can be included is limited? Further, can defect population be included in the calculations?

D. G. Pettifor. The sensitivity of planar fault energies to alloying additions is already being modelled. As the interatomic potentials become more realistic and computers ever more powerful, we can expect that modelling will be able to provide new insight into the role of alloying additions and non-stoichiometry on mechanical properties.

R. W. Cahn (*University of Cambridge, UK*). Professor Pettifor showed, for certain intermetallic phases, that the energy differences between the stable and the next-most-favourable crystal structures are exceedingly small. Can he reliably predict which of such phases will exhibit stacking faults (polytypism), like SiC or Co?

D. G. Pettifor. Yes, even though the absolute energy may show sizeable error, relative energies are usually very reliable. The polytypism in SiC or Co has been successfully predicted by groups in the Cavendish Laboratory and the Techniche Hochschule in Darmstadt.

PHILOSOPHICAL TRANSACTIONS OF THE ROYAL SOCIETY A MATHEMATICAL, PHYSICAL & ENGINEERING SCIENCES